[文章编号] 1671-587X(2025)06-1498-10 DOI:10.13481/j.1671-587X.20250606

表儿茶素对对乙酰氨基酚诱导小鼠肝损伤的改善作用及其机制

于蕙源[1,2]，金 令[3]，于 颖[4]，王 雪[5]，王 冰[6]

（1. 吉林大学第一医院放疗科，吉林 长春 130021；2. 吉林大学动物医学学院临床兽医学系，吉林 长春 130062；3. 吉林大学第一医院检验科，吉林 长春 130021；4. 吉林大学第一医院生殖中心产前诊断中心，吉林 长春 130021；5. 吉林省松原市吉林油田医院检验科，吉林 松原 138000；6. 吉林省肿瘤医院放疗科，吉林 长春 130012）

[摘 要] **目的：**探讨表儿茶素（EC）对对乙酰氨基酚（APAP）诱导小鼠肝损伤的改善作用，并阐明其可能的作用机制。**方法：**将60只C57BL/6J小鼠随机分为空白对照组、APAP模型组、低剂量（10 mg·kg^{-1}）EC组、中剂量（20 mg·kg^{-1}）EC组和高剂量（40 mg·kg^{-1}）EC组，每组12只。除空白对照组外，其余各组小鼠给予腹腔注射APAP（200 mg·kg^{-1}）诱导肝损伤模型。APAP注射前1 h，低、中和高剂量EC组小鼠腹腔分别注射10、20和40 mg·kg^{-1} EC。36只核因子E2相关因子2（Nrf2）缺陷小鼠（Nrf2$^{-/-}$小鼠）随机分为对照组、APAP组和APAP+EC组，每组12只。造模24 h后处死小鼠，收集小鼠血液和肝组织用于后续检测。采用HE染色观察各组小鼠肝组织病理形态表现，试剂盒检测各组小鼠血清中天冬氨酸氨基转移酶（AST）和丙氨酸氨基转移酶（ALT）活性及小鼠肝组织中髓过氧化物酶（MPO）活性和肿瘤坏死因子α（TNF-α）、白细胞介素1β（IL-1β）、丙二醛（MDA）、三磷酸腺苷（ATP）、谷胱甘肽（GSH）及亚铁离子（Fe^{2+}）水平，Western blotting法检测各组小鼠肝组织中核因子κB（NF-κB）和Nrf2信号通路相关蛋白表达水平。**结果：**HE染色，与APAP模型组比较，不同剂量EC组APAP诱导小鼠肝病理损伤明显改善。与空白对照组比较，APAP模型组小鼠血清中ALT和AST活性明显升高（$P<0.01$）；与APAP模型组比较，低、中和高剂量EC组小鼠血清中ALT及AST活性明显降低（$P<0.05$或$P<0.01$）。与空白对照组比较，APAP模型组小鼠肝组织中MPO活性及TNF-α和IL-1β水平明显升高（$P<0.01$）；与APAP模型组比较，低、中和高剂量EC组小鼠肝组织中MPO活性及TNF-α和IL-1β水平明显降低（$P<0.05$或$P<0.01$）。与空白对照组比较，APAP模型组小鼠肝组织中MDA和Fe^{2+}水平明显升高（$P<0.05$），ATP和GSH水平明显降低（$P<0.05$）；与APAP模型组比较，低、中和高剂量小鼠肝组织中MDA和Fe^{2+}水平明显降低（$P<0.05$或$P<0.01$），ATP和GSH水平明显升高（$P<0.05$或$P<0.01$）。与空白对照组比较，APAP模型组小鼠肝组织中氨基酸交换转运蛋白（xCT）和谷胱甘肽过氧化物酶4（GPX4）蛋白表达水平明显降低（$P<0.05$）；与APAP模型组比较，低、中和高剂量小鼠肝组织中xCT和GPX4蛋白表达水平明显升高（$P<0.01$）。与空白对照组比较，APAP模型组小鼠肝组织中核因子κB（NF-κB） p-p65和磷酸化NF-κB抑制剂α（p-IκBα）蛋白表达水平明显升高（$P<0.05$）；与APAP模型组比较，低、中和高剂量EC组小鼠肝组织中NF-κB p-p65和p-IκBα蛋白表达水平明显降低（$P<0.01$）。与空白对照组比较，APAP模型组小鼠肝组织中Nrf2和血清素加氧酶1（HO-1）蛋白水平明显升高（$P<0.05$）；与APAP模型组比较，低、中和高剂量EC组小鼠肝组织中Nrf2和HO-1蛋白水平明显升高（$P<0.01$）。与对照组比较，APAP组Nrf2$^{-/-}$小鼠血清中AST和ALT活性及肝组织中MDA和Fe^{2+}水平明显升高（$P<0.01$），肝组织中ATP和GSH

[收稿日期] 2024-12-09 [录用日期] 2025-01-16

[基金项目] 吉林省教育厅科研重点项目（JJKH20241337KJ）

[作者简介] 于蕙源（1998－），男，吉林省长春市人，在读硕士研究生，主要从事放射肿瘤学方面的研究。

[通信作者] 王 冰，副主任医师（E-mail：zisu8688@163.com）

水平明显降低（$P<0.01$）。**结论：**EC对APAP诱导的小鼠肝损伤具有改善作用，其机制可能与EC激活Nrf2/GPX4信号通路抑制铁死亡有关。

[关键词] 表儿茶素；对乙酰氨基酚；肝损伤；铁死亡；核因子E2相关因子2
[中图分类号] R575 [文献标志码] A

Improvement effect of epicatechin on liver injury in mice induced by acetaminophen and its mechanism

YU Huiyuan[1,2], JIN Ling[3], YU Ying[4], WANG Xue[5], WANG Bing[6]
(1. Department of Radiotherapy, First Hospital, Jilin University, Changchun 130021, China; 2. Department of Clinical Veterinary Medicine, School of Veterinary Medicine, Jilin University, Changchun 130062, China; 3. Department of Clinical Laboratory, First Hospital, Jilin University, Changchun 130021, China; 4. Reproductive Center, Prenatal Diagnosis Center, First Hospital, Jilin University, Changchun 130021, China; 5. Department of Clinical Laboratory, Songyuan Jilin Oilfield Hospital, Jilin Province, Songyuan 138000, China; 6. Department of Radiotherapy, Tumor Hospital, Jilin Province, Changchun 130012, China)

ABSTRACT **Objective:** To discuss the improvement effect of epicatechin(EC) on acetaminophen(APAP)-induced liver injury in the mice, and to clarify its possible mechanism. **Methods:** A total of 60 C57BL/6J mice were randomly divided into blank control group, APAP model group, low dose of EC group (10 $mg\cdot kg^{-1}$), middle dose of EC group (20 $mg\cdot kg^{-1}$) and high dose of EC group (40 $mg\cdot kg^{-1}$), with 12 mice in each group. Except for blank control group, the mice in the other groups were given intraperitoneal injection of APAP (200 $mg\cdot kg^{-1}$) to establish the liver injury models. At 1 h before APAP injection, the mice in low, middle and high doses of EC groups were intraperitoneally injected with 10, 20 and 40 $mg\cdot kg^{-1}$ EC, respectively. A total of 36 nuclear factor E2-related factor 2 (Nrf2) deficient mice ($Nrf2^{-/-}$ mice) were randomly divided into control group, APAP group and APAP+EC group, with 12 mice in each group. After modeling 24 h, the mice were sacrificed, and the blood and liver tissue of the mice were collected for subsequent detection. HE staining was used to observe the pathomorphology of the liver tissue in the mice in various groups; kit assay was used to detect the activities of aspartate aminotransferase (AST) and alanine aminotransferase (ALT) in serum of the mice in various groups and the myeloperoxidase (MPO) activity and the levels of tumor necrosis factor-α (TNF-α), interleukin-1β (IL-1β), malondialdehyde (MDA), adenosine triphosphate (ATP), glutathione (GSH) and ferrous ion (Fe^{2+}) in liver tissue of the mice in various groups; Western blotting method was used to detect the expression levels of nuclear factor-κB (NF-κB) and Nrf2 signaling pathway-related proteins in liver tissue of the mice in various groups. **Results:** The HE staining results showed that compared with APAP model group, the APAP-induced liver pathology injury in the mice in different doses of EC groups was significantly improved. Compared with blank control group, the levels of ALT and AST in serum of the mice in APAP model group were significantly increased ($P<0.01$). Compared with APAP model group, the activities of ALT and AST in serum of the mice in low, middle and high doses of EC groups were significantly decreased ($P<0.05$ or $P<0.01$). Compared with blank control group, the MPO activity and the levels of TNF-α and IL-1β in liver tissue of the mice in APAP model group were significantly increased ($P<0.01$). Compared with APAP model group, the MPO activity and the levels of TNF-α and IL-1β in liver tissue of the mice in low, middle and high doses of EC groups were decreased ($P<0.05$ or $P<0.01$). Compared with blank control group, the levels of MDA and Fe^{2+} in liver tissue of the mice in APAP model group were significantly increased ($P<$

0.05), and the levels of ATP and GSH were significantly decreased ($P<0.05$). Compared with APAP model group, the levels of MDA and Fe^{2+} in liver tissue of the mice in low, middle and high doses of EC groups were significantly increased ($P<0.05$ or $P<0.01$), and the levels of ATP and GSH were significantly increased ($P<0.01$). Compared with blank control group, the expression levels of amino acid exchange transporter (xCT) and glutathione peroxidase 4 (GPX4) proteins in liver tissue of the mice in APAP model group were significantly decreased ($P<0.05$); compared with APAP model group, the expression levels of xCT and GPX4 proteins in liver tissue of the mice in low, middle and high doses of EC groups were significantly increased ($P<0.01$). Compared with blank control group, the expression levels of nuclear factor-κB (NF-κB) p-p65 and phosphorylated NF-κB inhibitor α (p-IκBα) proteins in liver tissue of the mice in APAP model group were significantly increased ($P<0.05$); compared with APAP model group, the expression levels of NF-κB p-p65 and p-IκBα proteins in liver tissue of the mice in low, middle and high doses of EC groups were significantly decreased ($P<0.01$). Compared with blank control group, the expression levels of Nrf2 and heme oxygenase-1 (HO-1) proteins in liver tissue of the mice in APAP model group were significantly increased ($P<0.05$); compared with APAP model group, the expression levels of Nrf2 and HO-1 proteins in liver tissue of the mice in low, middle and high doses of EC groups were significantly increased ($P<0.01$). Compared with control group, the ALT level in serum and the levels of MDA and Fe^{2+} in liver tissue of the $Nrf2^{-/-}$ mice in APAP group were significantly increased ($P<0.01$), and the levels of ATP and GSH in liver tissue were significantly decreased ($P<0.01$). **Conclusion**: EC can improve APAP-induced liver injury in the mice, and its mechanism may be related to the inhibition of ferroptosis by activating the Nrf2/GPX4 signaling pathway.

KEYWORDS Epicatechin; Acetaminophen; Liver injury; Ferroptosis; Nuclear factor E2-related factor 2

对乙酰氨基酚（acetaminophen，APAP）是一种广泛使用的解热镇痛药物。在不合理用药和一些意外因素的作用下，服用APAP可能导致肝损伤，严重肝损伤甚至可能导致急性肝功能衰竭[1]。目前，N-乙酰半胱氨酸（N-acetylcysteine，NAC）是临床上抢救APAP肝损伤患者的首选药物[2]。NAC是细胞内谷胱甘肽（glutathione，GSH）合成的重要前体，其通过促进GSH合成、降低活性氧（reactive oxygen species，ROS）水平并参与恢复三磷酸腺苷（adenosine triphosphate，ATP）能量供应来发挥解毒作用[3]。然而，NAC的治疗时间窗窄，可能出现恶心、呕吐和过敏等不良反应，限制了其临床应用[4]。因此，寻找一种安全有效的药物来减轻APAP引起的肝损伤具有重要意义。铁死亡是一种铁依赖性细胞死亡，其特征不同于已知的细胞死亡形式[5]。铁死亡主要特征是细胞内脂质过氧化物的积累和氧化还原失衡[6]。铁死亡在药物性肝损伤、酒精性肝病、非酒精性脂肪性肝炎、病毒性肝炎、肝纤维化和其他肝病中发挥重要作用[7-8]。铁死亡可作为APAP诱导的肝损伤的潜在治疗靶点[9]。表儿茶素（epicatechin，EC）是由绿茶中提取的一种天然黄酮类化合物，由于其抗炎和抗氧化作用，因此对许多疾病具有治疗作用[10-11]。EC可通过减轻核因子κB（nuclear factor-κB，NF-κB）和丝裂原活化蛋白激酶（mitogen-activated protein kinase，MAPK)活化抑制脂多糖（lipopolysaccharide，LPS）诱导的肺损伤[12]。EC可通过NF-κB和NOD样受体家族Pyrin域蛋白3（NOD-like receptor family Pyrin domain containing protein 3，NLRP3）激活减轻炎症抑制痛风性关节炎[13]。EC减弱了LPS诱导的乳腺炎和牛乳腺上皮细胞中炎症因子的产生[14]。EC是否对APAP诱导的肝损伤具有保护作用目前尚未完全阐明。本研究探讨EC对APAP诱导小鼠肝损伤的保护作用，并阐明其作用机制，为治疗APAP诱导的肝损伤提供理论依据。

1 材料与方法

1.1 实验动物、主要试剂和仪器 60只SPF级C57BL/6J小鼠购自辽宁长生生物技术有限公司，实验动物生产许可证号：SCXK（辽）2020-0001。所有小鼠严格按照SPF级饲养条件喂养，饲养温度15 ℃～25 ℃，自由饮食饮水。EC（纯度＞98%）（货号：490-46-0）购自成都瑞芬思德丹生物科技有限公司，APAP（货号：AS511450）购自美国Sigma公司，天冬氨酸氨基转移酶（aspartate

aminotransferase，AST）（货号：ml095196）和丙氨酸氨基转移酶（alanine aminotransferase，ALT）（货号：ml095164）检测试剂盒购自上海酶联生物有限公司，肿瘤坏死因子α（tumor necrosis factor-α，TNF-α）（货号：430904）和白细胞介素1β（interleukin-1β，IL-1β）（货号：432604）酶联免疫吸附试验（enzyme linked immunosorbent assay，ELISA）试剂盒购自美国Biolegend公司，髓过氧化物酶（myeloperoxidase，MPO）（货号：A044-1-1）、丙二醛（malondialdehyde，MDA）（货号：A003-1-2）、ATP（货号：A095-1-1）、GSH（货号：A005-1-2）和亚铁离子（ferrous ions，Fe^{2+}）（货号：A039-2-1）检测试剂盒购自南京建成生物制剂有限公司，NF-κB（货号：#8242）和核因子E2相关因子2（nuclear factor erythroid 2-related factor 2，Nrf2）（货号：#33649）信号通路抗体以及NK-κB抑制剂α（inhibitor of NF-κB α，IκBα）抗体（货号：#4812）、磷酸化IκBα（phosphorylated IκBα，p-IκBα）抗体（货号：#2859）和血红素加氧酶1（heme oxygenase-1，HO-1）抗体（货号：#43966）购自美国CST公司。全自动酶标仪（型号：ELX800）购自美国Bio-Tek公司，全自动显微镜（型号：SMZ645）购自日本Nikon公司，转膜仪（型号：GelDoc Go）和蛋白凝胶成像仪（型号：GelDoc XR＋）购自美国Bio-Rad公司，电泳仪（型号：JC600D）购自北京六一仪器厂。

1.2 实验动物分组和给药 60只C57BL/6J小鼠随机分为空白对照组、APAP模型组、低剂量（10 mg·kg^{-1}）EC组、中剂量（20 mg·kg^{-1}）EC组和高剂量（40 mg·kg^{-1}）EC组，每组12只。空白对照组小鼠给予等体积的磷酸盐缓冲液（phosphate buffer saline，PBS），APAP模型组小鼠腹腔注射APAP（200 mg·kg^{-1}），低、中和高剂量EC组小鼠在APAP注射前1 h分别腹腔注射10、20和40 mg·kg^{-1} EC。Nrf2缺陷小鼠（Nrf2$^{-/-}$小鼠）购自美国缅因州巴尔港杰克逊实验室，来源于129×B6 F1背景，通过与C57B6/J种系杂交超过6代获得。36只Nrf2$^{-/-}$小鼠随机分为对照组、APAP组和APAP＋EC组，每组12只。对照组：小鼠接受等体积的PBS缓冲液，APAP组：小鼠腹腔注射APAP（200 mg·kg^{-1}），APAP＋EC组：小鼠在注射APAP前1 h腹腔注射EC（40 mg·kg^{-1}）。所有动物实验均经吉林大学基础医学院动物伦理委员会批准（审批号：2022142）。造模24 h后处死小鼠，收集小鼠血液和肝组织，用于后续实验。

1.3 HE染色观察各组小鼠肝组织病理形态表现 收取各组小鼠肝组织后，用4%多聚甲醛固定，经梯度乙醇脱水、二甲苯透明、石蜡包埋后制备石蜡切片。脱蜡和水合后，用HE染色试剂盒进行染色。最后，在光学显微镜下观察各组小鼠肝组织病理形态表现。

1.4 采用试剂盒检测各组小鼠血清中AST和ALT活性 将血液样本以3 000 r·min^{-1}离心15 min，分离血清。按照试剂盒说明书检测各组小鼠血清中AST和ALT活性。

1.5 采用试剂盒检测各组小鼠肝组织中MDA、ATP、GSH和Fe^{2+}水平 取适量小鼠肝组织样本，置于研磨器中。随后，加入适量的PBS缓冲液，并在冰浴条件下进行充分研磨制成匀浆，使用试剂盒检测各组小鼠肝组织匀浆中MDA、ATP、GSH和Fe^{2+}水平。

1.6 采用试剂盒检测各组小鼠肝组织中MPO活性及TNF-α和IL-1β水平 将各组小鼠肝组织与PBS缓冲液（1∶9）混合并在冰上研磨以获得上清液。根据试剂盒说明书检测各组小鼠肝组织中MPO活性及TNF-α和IL-1β水平。

1.7 Western blotting法检测各组小鼠肝组织中NF-κB和Nrf2信号通路相关蛋白及谷胱甘肽过氧化物酶4（glutathione peroxidase 4，GPX4）和氨基酸交换转运蛋白[system Xc-（cystine/glutamate antiporter），xCT]表达水平 各组小鼠肝组织置于冰的RIPA裂解缓冲液中裂解，在4 ℃、12 000 r·min^{-1}离心10 min。使用BCA测定试剂盒检测总蛋白浓度。将相同量的总蛋白于12%十二烷基磺酸钠-聚丙烯酰胺凝胶电泳（sodium dodecyl sulfate-polyacrylamid gel electrophoresis，SDS-PAGE）中电泳，随后转移至聚偏二氟乙烯（polyvinylidene fluoride，PVDF）膜上。用5%的脱脂乳封闭膜2 h后，在4 ℃下用一抗孵育过夜。将膜洗涤3次，每次10 min，在室温下与适当的辣根过氧化物酶偶联的二抗孵育1 h。使用增强化学发光系统测量免疫反应蛋白。使用Image J软件分析蛋白免疫印记条带，计算目的蛋白表达水平。目的蛋白表达水平＝目的蛋白条带灰度值/内参蛋白条带灰度值。

1.8 统计学分析 采用GraphPad Prism 9.0软件

进行统计学分析。各组小鼠血清中AST和ALT活性，各组小鼠肝组织中MPO活性以及TNF-α、IL-1β、MDA、GSH和Fe^{2+}水平，各组小鼠肝组织中NF-κB和Nrf2信号通路相关蛋白及xCT和GPX4蛋白表达水平均符合正态分布且方差齐，以$\bar{x}\pm s$表示，多组间样本均数比较采用单因素方差分析，组间样本均数两两比较采用LSD-t检验。以$P<0.05$为差异有统计学意义。

2 结 果

2.1 各组小鼠肝组织病理形态表现 空白对照组小鼠肝细胞排列紧密，肝窦未见明显扩张或挤压，也未观察到明显的炎症变化，见图1A；APAP模型组小鼠肝组织大面积坏死，大量肝细胞核固缩、深染、碎裂或溶解，伴有粒细胞浸润，见图1B；低剂量EC组小鼠肝组织出现坏死，肝细胞核固缩、深染、碎裂或溶解，伴有粒细胞浸润，见图1C；中剂量EC组小鼠肝组织出现肝细胞核固缩、深染，伴有少量炎性细胞浸润，见图1D；高剂量EC组小鼠肝组织和肝窦未见明显扩张或挤压，可观察到轻微的炎症变化。见图1E。

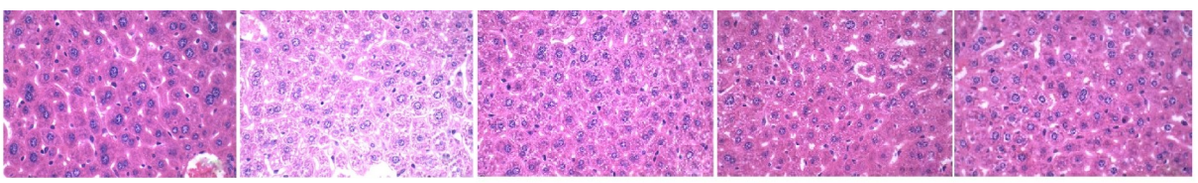

A B C D E

A：Blank control group；B：APAP model group；C：Low dose of EC group；D：Middle dose of EC group；E：High dose of EC group.

图1 各组小鼠肝组织病理形态表现（HE，×400）

Fig. 1 Pathomorphology of liver tissue of mice in various groups (HE，×400)

2.2 各组小鼠血清中AST和ALT活性 与空白对照组比较，APAP模型组小鼠血清中ALT和AST活性明显升高（$P<0.01$）。与APAP模型组比较，低、中和高剂量EC组小鼠血清中ALT和AST活性明显降低（$P<0.05$或$P<0.01$）。见表1。

2.3 各组小鼠肝组织中MPO活性及TNF-α和IL-1β水平 与空白对照组比较，APAP模型组小鼠肝组织中MPO活性及TNF-α和IL-1β水平明显升高（$P<0.01$）。与APAP模型组比较，低、中和高剂量EC组小鼠肝组织中MPO活性及TNF-α和IL-1β水平明显降低（$P<0.05$或$P<0.01$）。见表2。

表1 各组小鼠血清中AST和ALT活性

Tab. 1 Activites of ALT and AST in serum of mice in varIous groups [$n=6$，$\bar{x}\pm s$，$\lambda_B/(U\cdot L^{-1})$]

Group	ALT	AST
Blank control	32.75±17.52	47.12±22.56
APAP model	582.63±36.32*	509.22±15.97*
EC		
Low dose	425.33±21.47△	396.55±10.29△
Middle dose	215.69±19.59△△	189.96±30.21△△
High dose	153.92±24.91△△	109.85±26.91△△

*$P<0.01$ *vs* blank control group；△$P<0.05$，△△$P<0.01$ *vs* APAP model group.

表2 各组小鼠肝组织中MPO活性及TNF-α和IL-1β水平

Tab. 2 Activities of MPO and levels of TNF-α and IL-1β in liver tissue of mice in various groups （$n=6$，$\bar{x}\pm s$）

Group	MPO activity[$\lambda_B/(U\cdot L^{-1})$]	TNF-α level [$\omega_B/(ng\cdot g^{-1})$]	IL-1β level [$\omega_B/(ng\cdot g^{-1})$]
Blank control	1.023±0.352	119.36±10.32	47.12±22.56
APAP model	5.336±1.096*	756.83±63.98*	509.22±15.97*
EC			
Low dose	4.589±0.966△	572.41±98.25△	396.55±10.29△
Middle dose	2.158±0.765△△	276.85±50.67△△	189.96±30.21△△
High dose	1.864±0.919△△	159.72±56.91△△	109.85±26.91△△

*$P<0.01$ *vs* blank control group；△$P<0.05$，△△$P<0.01$ *vs* APAP model group.

2.4 各组小鼠肝组织中MDA、ATP、GSH和Fe^{2+}水平 与空白对照组比较，APAP模型组小鼠肝组织中MDA和Fe^{2+}水平明显升高（$P<0.05$），ATP和GSH水平降低（$P<0.05$）；与APAPS模型组比较，低、中和高剂量EC组小鼠肝组织中MDA和Fe^{2+}水平明显降低（$P<0.05$或$P<0.01$），ATP和GSH水平明显升高（$P<0.05$或$P<0.01$）。见图2。

2.5 各组小鼠肝组织中xCT和GPX4蛋白表达水平 与空白对照组比较，APAP模型组小鼠肝组织中xCT和GPX4蛋白表达水平明显降低（$P<0.05$）；与APAP模型组比较，低、中和高剂量EC组小鼠肝组织中xCT和GPX4蛋白表达水平明显升高（$P<0.01$）。见图3。

2.6 各组小鼠肝组织中NF-κB p-p65和p-IκBα蛋白表达水平 与空白对照组比较，APAP模型组小鼠肝组织中NF-κB p-p65和p-IκBα蛋白表达水平明显升高（$P<0.05$）；与APAP模型组比较，低、中和高剂量EC组小鼠肝组织中NF-κB p-p65和p-IκBα蛋白表达水平明显降低（$P<0.01$）。见图4。

2.7 各组小鼠肝组织中Nrf2和HO-1蛋白表达水平 与空白对照组比较，APAP模型组小鼠肝组织中Nrf2和HO-1蛋白表达水平明显升高（$P<0.05$）；与APAP模型组比较，低、中和高剂量EC组小鼠肝组织中Nrf2和HO-1蛋白表达水平明显升高（$P<0.01$）。见图5。

2.8 各组$Nrf2^{-/-}$小鼠肝组织病理形态表现 对照组$Nrf2^{-/-}$小鼠肝细胞排列紧密，肝窦未见明显扩张或挤压，也未观察到明显的炎症变化，见图6A；APAP组$Nrf2^{-/-}$小鼠肝组织大面积坏死，大量肝细胞核固缩、深染、碎裂或溶解，伴有粒细胞浸润，见图6B；APAP＋EC组小鼠肝组织出现坏死，肝细胞核固缩、深染、碎裂或溶解，伴有粒细胞浸润，见图6C。

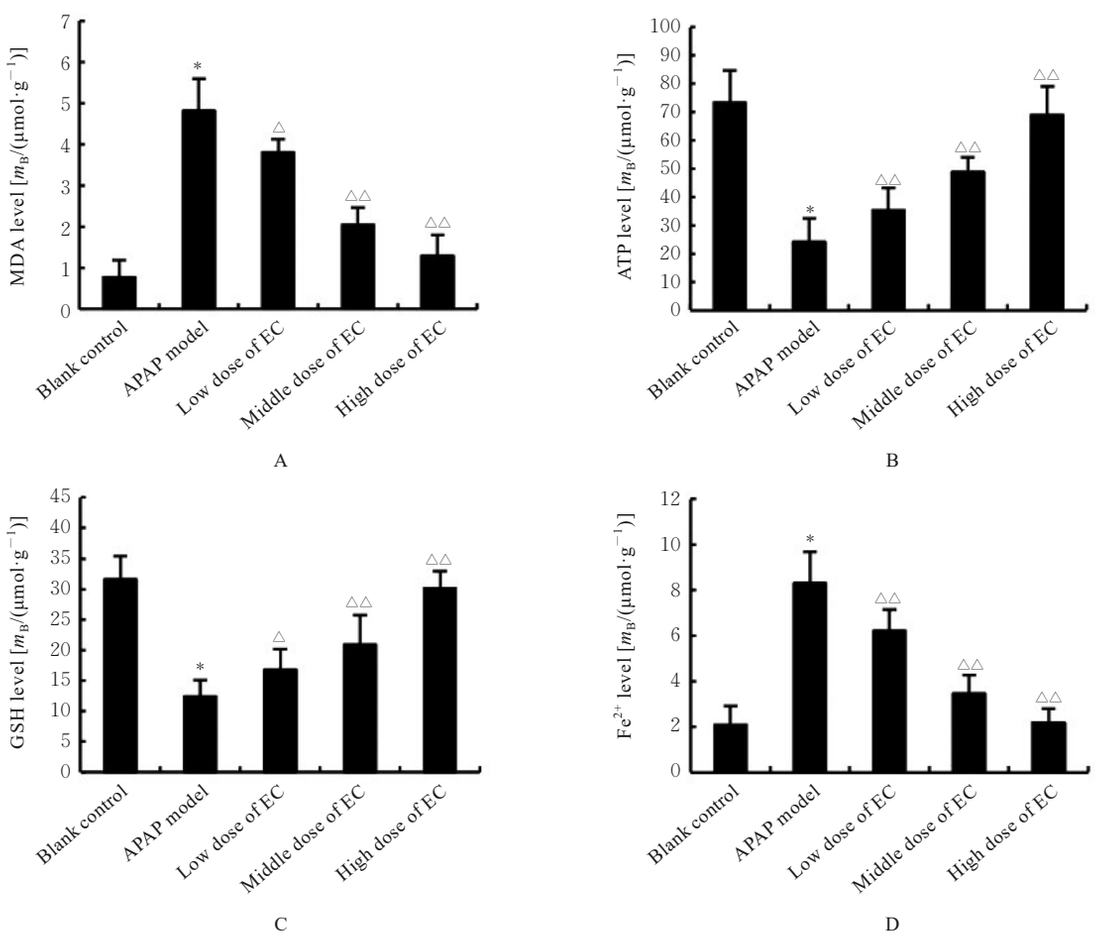

*$P<0.05$ *vs* blank control group; △$P<0.05$, △△$P<0.01$ *vs* APAP model group; A:MDA; B:ATP; C:GSH; D:Fe^{2+}.

图2 各组小鼠肝组织中MDA、ATP、GSH和Fe^{2+}水平

Fig. 2 Levels of MDA, ATP, GSH, and Fe^{2+} in liver tissue of mice in various groups

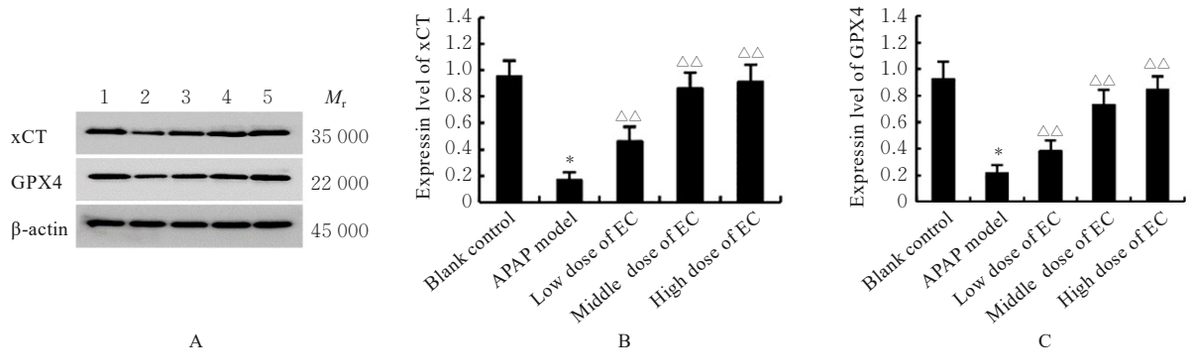

Lane 1: Blank control group; Lane 2: APAP model group; Lane 3－5: Low, middle, and high doses of EC groups. $^{*}P<0.05$ *vs* blank control group; $^{\triangle}P<0.05$, $^{\triangle\triangle}P<0.01$ *vs* APAP model group.

图 3 各组小鼠肝组织中 xCT 和 GPX4 蛋白表达电泳图(A)及直条图(B～C)

Fig. 3 Electrophoregram(A) and histograms(B－C) of expressions of GPX4 and xCT proteins in liver tissue of mice in various groups

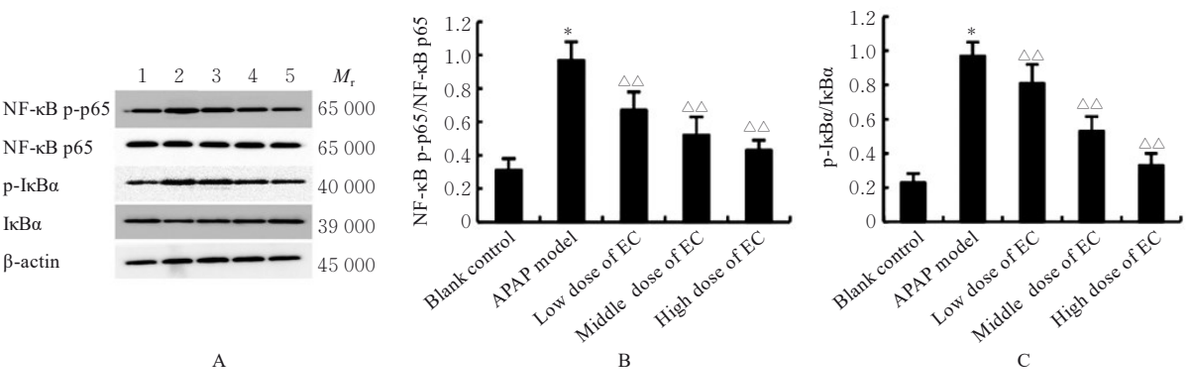

Lane 1: Blank control group; Lane 2: APAP model group; Lane 3－5: Low, middle, and high doses of EC groups. $^{*}P<0.05$ *vs* blank control group; $^{\triangle}P<0.05$, $^{\triangle\triangle}P<0.01$ *vs* APAP model group.

图 4 各组小鼠肝组织中 NF-κB p-p65 和 p-IκBα 蛋白表达电泳图(A)及直条图(B～C)

Fig.4 Electrophoregram(A) and histograms(B－C) of expressions of NF-κB p-p65 and p-IκBα proteins in liver tissue of mice in various groups

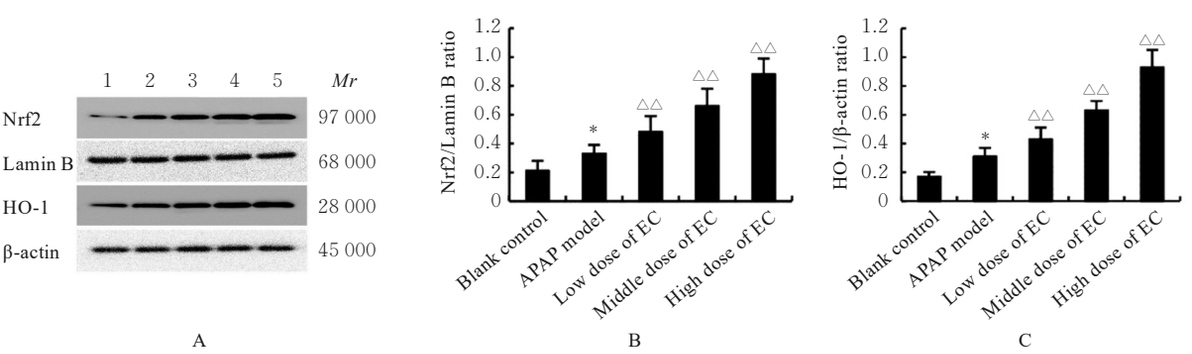

Lane 1: Blank control group; Lane 2: APAP model group; Lane 3－5: Low, middle, and high doses of EC groups. $^{*}P<0.05$ *vs* blank control group; $^{\triangle}P<0.05$, $^{\triangle\triangle}P<0.01$ *vs* APAP model group.

图 5 各组小鼠肝组织中 Nrf2 和 HO-1 蛋白表达电泳图(A)及直条图(B～C)

Fig. 5 Electrophoregram(A) and histograms(B－C) of expressions of Nrf2 and HO-1 proteins in liver tissue of mice in various groups

2.9 各组Nrf2$^{-/-}$小鼠血清中AST和ALT活性及肝组织中MDA、ATP、GSH和Fe^{2+}水平 与对照组比较，APAP组Nrf2$^{-/-}$小鼠血清中AST和ALT活性及肝组织中MDA和Fe^{2+}水平明显升高（$P<0.01$）；与APAP组比较，APAP＋EC组Nrf2$^{-/-}$小鼠血清中AST和ALT活性及肝组织中MDA和Fe^{2+}水平差异无统计学意义（$P>0.05$）。与对照组比较，APAP组Nrf2$^{-/-}$小鼠肝组织中ATP和GSH水平明显降低（$P<0.01$）；与APAP组比较，APAP＋EC组Nrf2$^{-/-}$小鼠肝组织中ATP和GSH水平差异无统计学意义（$P>0.05$）。见图7。

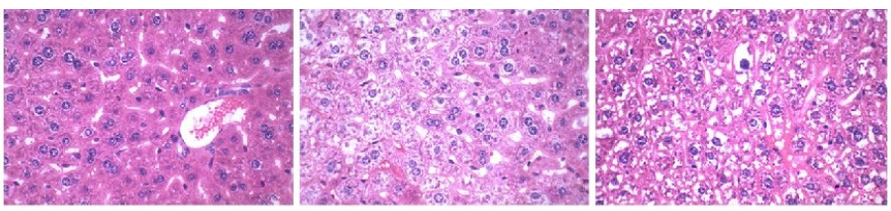

C：Control group; B：APAP group; C：APAP＋EC group.

图6 各组Nrf2$^{-/-}$小鼠肝组织病理形态表现（HE，×400）

Fig. 6 Pathomorphology of liver tissue of Nrf2$^{-/-}$ mice in various groups (HE, ×400)

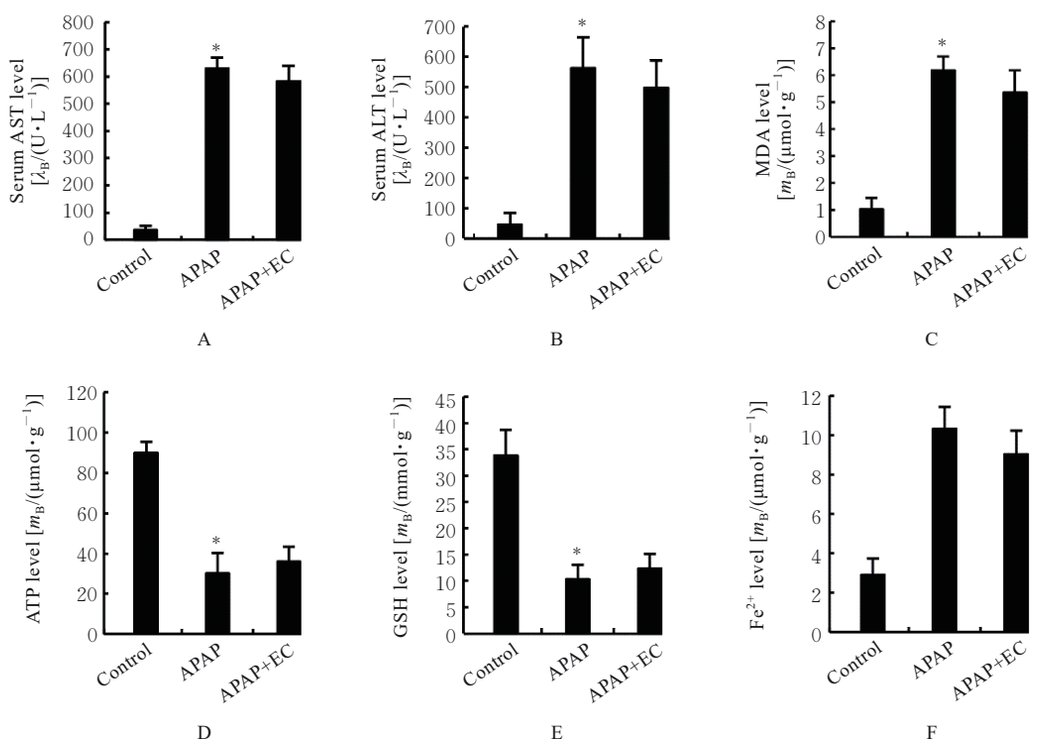

*$P<0.01$ *vs* control group.

图7 各组Nrf2$^{-/-}$小鼠血清中AST和ALT活性及肝组织中MDA、ATP、GSH和Fe^{2+}水平

Fig. 7 Activities of AST and ALT in serum and levels of MDA, ATP, GSH, and Fe^{2+} in liver tissue of Nrf2$^{-/-}$ mice in various groups

3 讨 论

炎症是肝损伤发病机制的关键因素[15]。研究[16-17]表明：在APAP诱导的肝损伤期间，驻留的肝库普弗细胞和募集的巨噬细胞在炎症中起着关键作用。APAP可增加巨噬细胞和中性粒细胞中炎症因子的释放[18]。上述炎症因子可诱导并加剧炎症，导致肝损伤[19]。MPO是中性粒细胞活化的标志物，其水平和活性代表着中性粒细胞的功能和状

态。NF-κB调节炎症因子的转录[20]。抑制NF-κB活化可以减轻APAP诱导的炎症和肝损伤，NF-κB可以作为防治APAP诱导肝损伤的潜在靶点[21]。因此，本研究检测EC对NF-κB信号通路的影响，结果显示：EC可以减弱APAP诱导的MPO活性的升高，促进TNF-α和IL-1β的产生及NF-κB的激活，进而发挥抗炎作用。

铁死亡是一种由脂质过氧化驱动的铁依赖性氧化细胞死亡，是区别于细胞凋亡、细胞自噬的新型细胞程序性死亡方式。各种抗氧化系统在预防脂质过氧化介导的铁死亡中起着重要作用，特别是胱氨酸/谷氨酸反向转运蛋白/GSH/GPX4轴系统[22]。研究[23]发现：APAP诱导小鼠肝损伤过程中存在铁死亡的发生，抑制铁死亡可以减轻APAP诱导的肝损伤，表明铁死亡可以作为肝损伤的靶点。本研究结果显示：EC可以抑制APAP诱导的MDA和Fe^{2+}的产生，同时上调ATP和GSH水平及GPX4和xCT的表达，表明EC可以抑制APAP诱导的肝铁死亡。

GPX4是一种脂质修复酶，也是铁死亡的主要调节因子[24]。GPX4的表达受Nrf2调控[25]。当受到外部氧化应激因子的刺激时，Nrf2及其抑制剂蛋白Keap1解离并激活，进入细胞核，开始其下游靶基因［超氧化物歧化酶（superoxide dismutase，SOD）、GPX4、xCT和HO-1］的表达，并发挥抗氧化作用[26-27]。Nrf2/HO-1信号通路在APAP诱导肝损伤的发展中起重要作用[28]。激活Nrf2/HO-1通路可以改善脂质功能障碍，保护APAP诱导的肝损伤[29-30]。研究[31]表明：激活Nrf2并上调GPX4的表达可以减少细胞中的氧化应激，并抑制GSH过氧化物酶4抑制剂RSL3诱导的成骨细胞铁死亡。这表明Nrf2/GPX4通路的激活可以抑制铁死亡。在本研究中，EC增加了Nrf2、HO-1和GPX4的表达，表明其可激活Nrf2信号通路。为进一步探讨EC对APAP诱导肝损伤的保护作用是否依赖于Nrf2信号通路，本研究利用$Nrf2^{-/-}$小鼠检测EC对APAP诱导肝损伤的保护作用，结果显示：在$Nrf2^{-/-}$小鼠中，EC对APAP诱导小鼠肝组织病理学变化、炎症因子和铁死亡的影响消失，表明EC对APAP诱导肝损伤的保护作用依赖于Nrf2。

综上所述，EC对APAP诱导的肝损伤具有改善作用，其机制可能与EC激活Nrf2/GPX4信号通路抑制铁死亡有关。

利益冲突声明：

所有作者声明不存在利益冲突。

作者贡献声明：

于蕙源参与实验设计和论文撰写，金令参与数据收集，于颖参与数据统计学分析，王雪参与文献查阅，王冰参与论文修改和审阅。

［参考文献］

[1] SIEMIONOW K, TEUL J, DRAGOWSKI P, et al. New potential biomarkers of acetaminophen-induced hepatotoxicity[J]. Adv Med Sci, 2016, 61(2): 325-330.

[2] WOODHEAD J L, HOWELL B A, YANG Y, et al. An analysis of N-acetylcysteine treatment for acetaminophen overdose using a systems model of drug-induced liver injury[J]. J Pharmacol Exp Ther, 2012, 342(2): 529-540.

[3] MORRIS G, ANDERSON G, DEAN O, et al. The glutathione system: a new drug target in neuroimmune disorders[J]. Mol Neurobiol, 2014, 50(3): 1059-1084.

[4] WALLACE K P, CENTER S A, HICKFORD F H, et al. S-adenosyl-L-methionine (SAMe) for the treatment of acetaminophen toxicity in a dog[J]. J Am Anim Hosp Assoc, 2002, 38(3): 246-254.

[5] YU H T, GUO P Y, XIE X Z, et al. Ferroptosis, a new form of cell death, and its relationships with tumourous diseases[J]. J Cell Mol Med, 2017, 21(4): 648-657.

[6] DIXON S J, LEMBERG K M, LAMPRECHT M R, et al. Ferroptosis: an iron-dependent form of nonapoptotic cell death[J]. Cell, 2012, 149(5): 1060-1072.

[7] CAPELLETTI M M, MANCEAU H, PUY H, et al. Ferroptosis in liver diseases: an overview[J]. Int J Mol Sci, 2020, 21(14): 4908.

[8] CHEN J Y, LI X P, GE C D, et al. The multifaceted role of ferroptosis in liver disease[J]. Cell Death Differ, 2022, 29(3): 467-480.

[9] WANG C, LIU T, TONG Y M, et al. Ulinastatin protects against acetaminophen-induced liver injury by alleviating ferroptosis via the SIRT1/NRF2/HO-1 pathway[J]. Am J Transl Res, 2021, 13(6): 6031-6042.

[10] LAN X, HAN X N, LI Q, et al. (-)-Epicatechin, a natural flavonoid compound, protects astrocytes against hemoglobin toxicity via Nrf2 and AP-1 signaling pathways[J]. Mol Neurobiol, 2017, 54(10): 7898-7907.

[11] TIAN X, XUE Y S, XIE G G, et al. (-)-Epicatechin ameliorates cigarette smoke-induced lung inflammation

via inhibiting ROS/NLRP3 inflammasome pathway in rats with COPD[J]. Toxicol Appl Pharmacol, 2021, 429: 115674.

[12] XING J, YU Z L, ZHANG X Y, et al. Epicatechin alleviates inflammation in lipopolysaccharide-induced acute lung injury in mice by inhibiting the p38 MAPK signaling pathway[J]. Int Immunopharmacol, 2019, 66: 146-153.

[13] WU C X, LI F F, ZHANG X X, et al. (-)-Epicatechin ameliorates monosodium urate-induced acute gouty arthritis through inhibiting NLRP3 inflammasome and the NF-κB signaling pathway[J]. Front Pharmacol, 2022, 13: 799552.

[14] MA X, LI M M, LU G C, et al. Anti-inflammation of epicatechin mediated by TMEM35A and TMPO in bovine mammary epithelial cell line cells and mouse mammary gland[J]. J Dairy Sci, 2021, 104(12): 12925-12938.

[15] TACKE F, LUEDDE T, TRAUTWEIN C. Inflammatory pathways in liver homeostasis and liver injury[J]. Clin Rev Allergy Immunol, 2009, 36(1): 4-12.

[16] YOU Q, HOLT M, YIN H, et al. Role of hepatic resident and infiltrating macrophages in liver repair after acute injury[J]. Biochem Pharmacol, 2013, 86(6): 836-843.

[17] HOLT M P, CHENG L L, JU C. Identification and characterization of infiltrating macrophages in acetaminophen-induced liver injury[J]. J Leukoc Biol, 2008, 84(6): 1410-1421.

[18] KRENKEL O, MOSSANEN J C, TACKE F. Immune mechanisms in acetaminophen-induced acute liver failure[J]. Hepatobiliary Surg Nutr, 2014, 3(6): 331-343.

[19] JAESCHKE H, DAVID WILLIAMS C, RAMACHANDRAN A, et al. Acetaminophen hepatotoxicity and repair: the role of sterile inflammation and innate immunity[J]. Liver Int, 2012, 32(1): 8-20.

[20] HAYDEN M S, GHOSH S. Regulation of NF-κB by TNF family cytokines[J]. Semin Immunol, 2014, 26(3): 253-266.

[21] LIU A M, TANAKA N, SUN L, et al. Saikosaponin d protects against acetaminophen-induced hepatotoxicity by inhibiting NF-κB and STAT3 signaling[J]. Chem Biol Interact, 2014, 223: 80-86.

[22] LAI Y F, DONG J, WU Y, et al. Lipid peroxides mediated ferroptosis in electromagnetic pulse-induced hippocampal neuronal damage via inhibition of GSH/GPX4 axis[J]. Int J Mol Sci, 2022, 23(16): 9277.

[23] YAMADA N, KARASAWA T, TAKAHASHI M. Role of ferroptosis in acetaminophen-induced hepatotoxicity[J]. Arch Toxicol, 2020, 94(5): 1769-1770.

[24] FORCINA G C, DIXON S J. GPX4 at the crossroads of lipid homeostasis and ferroptosis[J]. Proteomics, 2019, 19(18): e1800311.

[25] ZHU L J, CHEN D Z, ZHU Y, et al. GPX4-regulated ferroptosis mediates S100-induced experimental autoimmune hepatitis associated with the Nrf2/HO-1 signaling pathway[J]. Oxid Med Cell Longev, 2021, 2021(1): 6551069.

[26] PANIERI E, PINHO S A, AFONSO G J M, et al. NRF2 and mitochondrial function in cancer and cancer stem cells[J]. Cells, 2022, 11(15): 2401.

[27] PANG C, ZHENG Z Y, SHI L, et al. Caffeic acid prevents acetaminophen-induced liver injury by activating the Keap1-Nrf2 antioxidative defense system[J]. Free Radic Biol Med, 2016, 91: 236-246.

[28] LI H Y, WENG Q Q, GONG S, et al. Kaempferol prevents acetaminophen-induced liver injury by suppressing hepatocyte ferroptosis via Nrf2 pathway activation[J]. Food Funct, 2023, 14(4): 1884-1896.

[29] CAI X P, HUA S Y, DENG J W, et al. Astaxanthin activated the Nrf2/HO-1 pathway to enhance autophagy and inhibit ferroptosis, ameliorating acetaminophen-induced liver injury [J]. ACS Appl Mater Interfaces, 2022, 14(38): 42887-42903.

[30] LI L, HUANG W X, WANG S K, et al. Astragaloside Ⅳ attenuates acetaminophen-induced liver injuries in mice by activating the Nrf2 signaling pathway [J]. Molecules, 2018, 23(8): 2032.

[31] PARK T J, PARK J H, LEE G S, et al. Quantitative proteomic analyses reveal that GPX4 downregulation during myocardial infarction contributes to ferroptosis in cardiomyocytes[J]. Cell Death Dis, 2019, 10(11): 835.